Comparison of three methods for estimating the sea level rise effect on storm surge flooding

Some of the authors of this publication are also working on these related projects:

Assessment of Hydrodynamic and Water Quality Impacts for Channel Deepening in the Thimble Shoals, Norfolk Harbor, and Elizabeth River Channels View project

Create new project "Applications of LIDAR data" View project

Comparison of three methods for estimating the sea level rise effect on storm surge flooding

**Keqi Zhang · Yuepeng Li · Huiqing Liu ·
Hongzhou Xu · Jian Shen**

Abstract Two linear methods, including the simple linear addition and linear addition by expansion, and numerical simulations were employed to estimate storm surges and associated flooding caused by Hurricane Andrew for scenarios of sea level rise (SLR) from 0.15 m to 1.05 m with an interval of 0.15 m. The interaction between storm surge and SLR is almost linear at the open Atlantic Ocean outside Biscayne Bay, with slight reduction in peak storm surge heights as sea level rises. The nonlinear interaction between storm surges and SLR is weak in Biscayne Bay, leading to small differences in peak storm surge heights estimated by three methods. Therefore, it is appropriate to estimate elevated storm surges caused by SLR in these areas by adding the SLR magnitude to storm surge heights. However, the magnitude and extent of inundation at the mainland area by Biscayne Bay estimated by numerical simulations are, respectively, 22–24 % and 16–30 % larger on average than those generated by the linear addition by expansion and the simple linear addition methods, indicating a strong nonlinear interaction between storm surge and SLR. The population and property affected by the storm surge inundation estimated by numerical simulations differ up to 50–140 % from that estimated by two linear addition methods. Therefore, it is inappropriate to estimate the exacerbated magnitude and extent of storm surge flooding and affected population and property caused by SLR by using the linear addition methods. The strong nonlinear interaction between surge flooding and SLR at a specific location occurs at the initial stage of SLR when the water depth under an elevated sea level is less than 0.7 m, while the interaction becomes linear as the depth exceeds 0.7 m.

K. Zhang
Department of Earth and Environment, Florida International University, Miami, FL 33199, USA

K. Zhang (✉) · Y. Li · H. Liu · H. Xu
International Hurricane Research Center, Florida International University, Miami, FL 33199, USA
e-mail: zhangk@fiu.edu

J. Shen
Virginia Institute of Marine Science, College of William and Mary, Gloucester Point, VA 23062, USA

1 Introduction

Low-lying coastal areas along the U.S. Atlantic and Gulf Coasts are vulnerable to flooding caused by storm surge and sea level rise (SLR). The 2007 IPCC report projects a global SLR of 0.18–0.59 m by 2100 according to various scenarios for future climate changes (Bindoff et al. 2007). However, the IPCC projection does not include the effect of the acceleration in melting of Antarctic and Greenland ice sheets on SLR, leading to a potential underestimate of future SLR. Rahmstorf (2007) and Vermeer and Rahmstorf (2009) estimated that sea level could rise by 1.4–1.9 m by 2100 using the empirical relationship between the increase in global temperature and the SLR rate based on time series from 1880 to 2000. The U.S. Army Corps of Engineers projected a global SLR of 1.0–1.5 m by 2100 by updating the estimates from the National Research Council's report in 1987 (National Research Council 1987; U.S. Army Corps of Engineers 2011). Recently, Katsman et al. (2011) have developed a SLR scenario of 0.55 to 1.15 m by 2100 by estimating high-end contributions of each of the components influencing global sea level changes. Such SLRs in this century would greatly exacerbate the threat from storm surge flooding; thus, the SLR effects on storm surges need to be quantified in order to cope with the impacts from climate changes on coastal areas.

A straightforward way to account for the SLR effect on storm surge flooding is to simply add the magnitudes of SLRs to storm surge heights. For example, Wu et al. (2002) estimated the increase in surge flood risk induced by SLRs along the coast of Cape May County in New Jersey by adding various magnitudes of SLRs to storm surges generated by the Sea, Lake and Overland Surges from Hurricanes (SLOSH) model (Jelesnianski et al. 1992). Following the same line of thinking, Kleinosky et al. (2007) estimated the changes of vulnerability to storm surge flooding in Hampton Roads, Virginia as a result of SLR. Additionally, Frazier et al. (2010) evaluated the impacts of storm surges together with SLR on the coast of Sarasota County in Florida and Shepard et al. (2011) quantified the effects of SLR on storm surge risk for the southern shores of Long Island, New York. The implicit assumption of the linear addition method is that the inundation dynamics of storm surges with an elevated sea level is the same as the dynamics with the current sea level by ignoring the nonlinear interaction between SLR and storm surge. However, the interaction between SLR and storm surge can be significant in the shallow water because the bottom friction and advective terms in the momentum equation for storm surge change nonlinearly as water depths increase, types of bottom covers alter, and shoreline configurations change. A more appropriate way to estimate the effect of SLR on surge inundation is to include SLR into the dynamic modeling of storm surge.

The early studies on dynamic modeling of the interaction between storm surge and SLR was conducted on coarse resolution grids covering large oceanic areas such as the North Sea without involving wetting and drying processes of surge flooding (De Ronde 1993; Flather and Williams 2000). The results showed that SLR caused small changes in storm surge heights in the open ocean if wind velocities remained unchanged. Recently, Lin et al. (2012) have estimated the SLR effect on the risk of hurricane storm surge for New York City by incorporating SLR into storm surge models capable of simulating inundation. Smith et al. (2010) investigated the effects of 0.5 and 1.0 m of SLR on storm surge and waves along the Louisiana Coast in terms of six hypothetic hurricanes. It was found that the surge level increased almost linearly with SLR in the maximum peak surge areas, but the surge level in the wetland areas of moderate peak surges increased by as much as 1–3 m in addition to the magnitudes of SLR. Mousavi et al. (2011) showed that the peak surge from Hurricane Beulah in 1967 with SLR was higher than that without SLR along the east side of Corpus Christi Bay, Texas, while the peak surge with SLR was lower than that without SLR along

the west side. These studies demonstrated that there were nonlinear interactions between SLR and storm surge; however, the effect of nonlinear interaction on the magnitude and extent of surge flooding has not been investigated systematically. Additionally, the differences between the linear addition method and the numerical simulation method in depicting the inundation of storm surge with SLR have not been evaluated. The linear superimposition of water level increases due to storm surge and SLR, respectively, is easy to implement and efficient in computation, while conducting hydrodynamic simulations need more computational efforts. Whether the linear addition method can produce an inundation pattern similar to that by numerical modeling is critical to appropriately and efficiently quantify exacerbation of surge flooding caused by SLR.

The densely populated Atlantic Coast of South Florida with a low topographic relief is frequently impacted by hurricanes from both the Atlantic Ocean and the Gulf Mexico. This coast provides an ideal location to examine the interaction between storm surge and SLR, and its effect on coastal population and property. The objectives of this research are (1) to examine the interaction between storm surge and SLR along the Atlantic Coast of South Florida and (2) to compare the difference between the linear addition and numerical simulation methods in calculating the magnitudes and extents of storm surge inundation and its effects on the estimation of the coastal population and real property exposed to storm surge flooding. The remainder of the paper is arranged as follows: Section 2 describes the study area; Section 3 presents the methods for computing storm surges with SLR; Section 4 provides the results; Section 5 presents the discussion; Sections 6 lists conclusions.

2 Study area

The SLOSH's Miami grid (basin), covering 8,000 km^2 of Atlantic coastal areas in St. Lucie, Martin, Palm Beach, Broward, Miami Dade, and Monroe Counties, served as the study area of this research (Fig. 1). There are more than 5 million people and approximately one trillion dollars of real property in this basin, according to 2010 census data and 2007 property tax data from the Florida Department of Revenue (Zhang 2011). The narrow continental shelf next to the South Florida Coast restricts the generation of high storm surges; however, the large area of shallow water inside and outside Biscayne Bay in Miami-Dade County provides a favorable condition to generate high storm surges along the coast next to Biscayne Bay. A relatively high topographic feature, the Atlantic Coastal Ridge with elevations of 3–6 m and widths of 5–10 km, extends from Martin County to mid-Miami-Dade County and diminishes in southern Miami-Dade County (Fig. 1). Most residential and commercial properties were developed on the Atlantic Coastal Ridge and in the low-lying areas east of the Ridge. Numerous streams and canals developed over the glades perpendicular to the Atlantic Coastal Ridge connect the Everglades marsh along the west side of the study area to the Atlantic Ocean along the east side.

The history of the development in the Miami Basin is a history of the interaction between humans and nature through cycles of building-destruction-rebuilding controlled by hurricane activities. Since 1850, four storms including hurricanes in 1888, 1926, 1945, and 1992 (Andrew) have generated severe damage to the built environment in the Miami Basin and caused high storm surge along the coastal area. The surge flooding records for the 1888, 1926, and 1945 hurricanes are in paucity and Hurricane Andrew is the only historical storm event with measured inundation magnitude and extent in the Miami Basin. Andrew's surges were also simulated by the Coastal and Estuarine Storm Tide (CEST) model that was validated with substantial field observations (Zhang et al. 2008). The root mean square
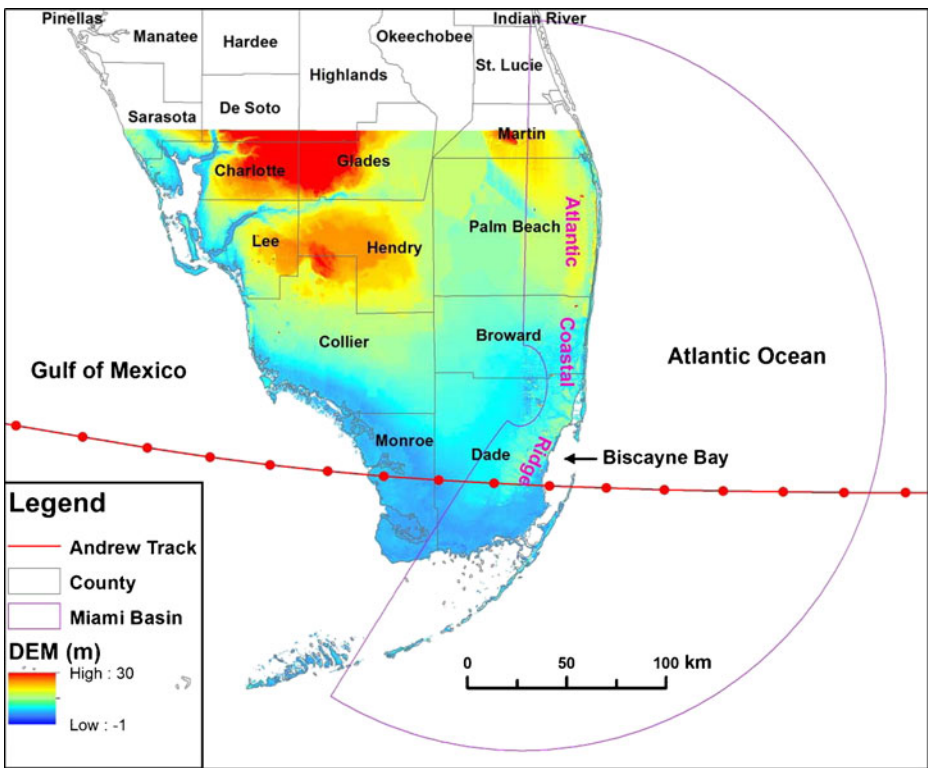
Fig. 1 The storm surge model basin, the digital elevation model of study area, and the track of Hurricane Andrew

difference between computed and observed maximum high water levels at more than 200 locations is about 0.44 m. There is also a good agreement between the computed inundation extent and the surveyed debris line left by Andrew's surge. Therefore, Andrew was selected as a representative case to investigate the interaction between SLR and storm surge.

3 Methods for computation of storm surge with sea level rise

The linear superimposition of SRL and storm surge, and dynamic simulation of storm surge with SLR are two often used methods for estimating storm surge flooding as sea level rises. Both methods were employed to compute storm surge with SLR for a comparison purpose.

3.1 Numerical simulation of storm surge with SLR

The CEST model (Supplemental Material, hereafter SM, Section 1) was employed to simulate storm surge under various SLR scenarios in the SLOSH's Miami basin. The semi-implicit, two-dimensional, depth-averaged CEST model operating over orthogonal curvilinear grids was used to simulate storm surge in this study. The Miami basin is an elliptical grid with a cell size of 0.6–0.7 km in coastal areas and a cell size of 2–3.5 km in the deep water about 150 km offshore. This grid was refined by reducing the edge size of a cell

by a factor of four in order to better represent the effect of linear features such as canals, streams, navigation channels, and coastal ridges on surge inundation (SM Section 2 and Fig. S1). The refined model grid is comprised of about 380,000 cells with sizes of 0.15–0.18 km in coastal areas. The following assumptions were made to facilitate the modeling of the interaction of SLR and storm surges using the CEST model.

3.1.1 Assumptions for modeling storm surges with SLR

First, in addition to inundation, the shorelines in South Florida are continuously altered by erosion and accretion processes as sea level rises (Zhang et al. 2004). Since it is difficult to predict the shoreline changes caused by erosion and accretion processes at a specific location, it is assumed that the topography of the study area remains unchanged in the future. This assumption is somewhat reasonable for South Florida because of a lack of significant sediment inputs to the coast for accretion. Additionally, surface sediments on the barrier islands and the Biscayne Bay Coast are thin and the underlying Anastasia Formation composed of sands and coquinoid limestones (Davis 1997; Finkl and Warner 2005) is difficult to erode. Shore protection measures that may be taken in the future can also alter inundation dynamics, but are difficult to include into the inundation analysis due to uncertainty in their form and extent. Therefore, the future shoreline protection measures are also excluded from the storm surge simulation. Second, the distribution of the current land cover is assumed to remain unchanged except for the area that is inundated by the elevated sea level. The land cover type in the inundated area is changed into the ocean and the Manning bottom friction coefficient (Zhang et al. 2012) is set to be the same as that for the ocean cells.

3.1.2 Incorporation of SLR into CEST

The measurements from global positioning systems indicate that South Florida is tectonically stable (Sella et al. 2007). The local SLR rate for South Florida is about 2.2 mm/year in terms of water level records for the 20th century at Key West, which is close to the average global SLR rate of 1.8 mm/year (Douglas 2001). Thus, it is reasonable to assume that the future SLR rate for South Florida is the same as the global rate. Based on the global SLR scenarios developed by Katsman et al. (2011), a series of SLR scenarios (0, 0.15, 0.30, 0.45, 0.60, 0.75, 0.90, and 1.05 m referenced to NAVD 88) were employed to examine the SLR and surge interaction by numerical simulations. The utilization of multiple scenarios of SLR allows us to accommodate the uncertainty in future SLR projections and to analyze the SLR and surge interaction at the different stages of SLR. For a given scenario of SLR, the water depths and Manning bottom friction coefficients of the CEST model grid cells were updated based on an algorithm listed in SM Section 3 before conducting numerical simulations.

3.1.3 Setup for modeling storm surge

Both parametric models and time series of wind fields (H*Wind) with intervals of 2–5 h generated by the Hurricane Research Division of the National Oceanic and Atmospheric Administration (NOAA) based on field measurements (Powell et al. 1998, 2009) can be used to compute wind stresses. The parametric wind model used by the SLOSH model (Jelesnianski et al. 1992) was employed to estimate the hurricane wind field when H*Wind data were not available. The still water level was set up to be the same as the scenarios of sea level rise from 0 m to 1.05 m referenced to NAVD 88 with an interval of 0.15 m. The tidal component was not included into the simulations because of a small tide range in the study area (Zhang et al. 2008).

The wave contribution to storm surges was also excluded because waves are relatively small in the Miami basin due to the sheltering effect of Bahamas Islands. The wave contribution is further reduced inside Biscayne Bay, where high surge occurs in the Miami basin, because the barrier islands protect the shallow lagoon water from the influence of high-energy waves from the Atlantic Ocean. Manning bottom friction coefficients for the underwater portion of the basin were set to be 0.015. Manning coefficients for the land portion were calculated based on land cover categories by modifying the table proposed by Mattocks and Forbes (2008) (Table 1 in Zhang et al. 2012). Each simulation with a time step of 10s, starting at 11:00 coordinated universal time (UTC), 21 August 1992 and ending at 15:00 UTC, 25 August 1992, continued for 99 h.

3.2 Simple linear addition method

The linear superimposition of SLR and storm surge assumes that the surge dynamics remain unchanged with a rising sea level. Peak storm surge heights (PSSHs) under an elevated sea level are a simple addition of the SLR magnitude to the PSSHs which come from a base case simulation with the current sea level. However, the calculation of future PSSHs in the land area adjacent to the current inundated area is a challenging task. None of the publications using the simple linear addition method (Frazier et al. 2010; Kleinosky et al. 2007; Wu et al. 2002) clearly presented how storm surge heights in this portion were calculated. A straightforward way is to first find the low-lying land areas below the future sea level and set PSSHs in these areas to be equal to the height of the elevated sea level. Then, the low-lying areas connecting to the area inundated by base case surges are included into the area inundated by storm surges for the elevated sea level using a method similar to Algorithm 1 in SM Section 3. The problem of this method is that base case PSSHs in the wet cells next to dry cells are not zero in many cases because of the complicated interaction among surge flows, topographic features, and land covers. An abrupt jump may occur between the elevated PSSHs in the area inundated by base case surges and the PSSHs in the area inundated by a rising sea level, but not by base case surges.

3.3 Linear addition by expansion method

A more sophisticated way for the linear superimposition of SLR and storm surge is to determine the inundation of the land areas next to the wet and dry boundary of the current storm surge by gradually expanding wet cells using a method similar to that proposed by McInnes et al. (2011). The detailed linear addition by expansion algorithm can be found in SM Section 4. Both simple linear addition and linear addition by expansion methods were employed in this study to compare the difference between the linear addition and nonlinear dynamic coupled methods in combination of SLR and storm surge.

4 Results

The large values of computed PSSHs using the CEST model occur in the middle portion of Biscayne Bay to the right side of Hurricane Andrew's track (Fig. S2a in SM Section 5 and Fig. 2a). The values of PSSHs increase as the sea level rises (Figs. S2b and S2c) and the area with PSSHs of 2.9–3.2 m enlarges several times when the sea level reaches about 1.05 m above the current position. In order to examine the interaction between SLR and storm surge, the PSSH differences were computed by subtracting base case PSSHs for the current sea level and the magnitude of SLR from the PSSHs for an elevated sea level. For various
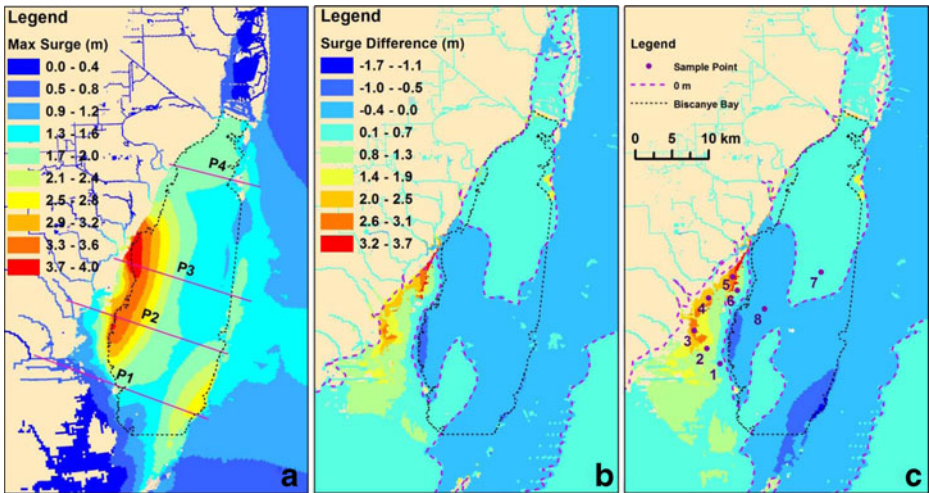
Fig. 2 **a** The PSSHs of Hurricane Andrew in Biscayne Bay and surrounding areas computed using the CEST model with the current sea level (base case). **b** The differences derived by subtracting the SLR magnitude and base case PSSHs from the PSSHs for the 0.6 m SLR. **c** The differences derived by subtracting the SLR magnitude and base case PSSHs from PSSHs with the 1.05 m SLR. The locations of sample points and four profiles in Figs. 3 and 4 are also displayed

SLR cases, PSSH differences should be zero if storm surge heights for elevated sea levels are simply linear additions of SLR magnitudes to base case storm surge heights. Figure 2b and c show that this is not always the case for the PSSH values in the area surrounding Biscayne Bay for SLR scenarios of 0.6 and 1.05 m.

In the case of the 0.6 m SLR, the PSSH differences in the open water outside Biscayne Bay are slightly below zero, except for the area towards the right corner outside Biscayne Bay where the PSSH differences are slightly larger than zero (Fig. 2b). Inside Biscayne Bay, the spatial distribution of PSSH differences exhibits irregular tongue shapes, with positive values in the northern portion and east of the southwest portion and negative values west of the southwest portion as well as the southeast portion. In the area in Biscayne Bay with PSSH values of greater than 2.9 m (Fig. 2a), the PSSH differences range from −0.6 m to −0.2 m, showing that the nonlinear interaction reduces the peak surge heights there by 7–20 %. In most water areas inside and outside Biscayne Bay, the values of PSSH differences are relatively small, ranging from −0.2 m to 0.2 m, except for a small area with values of −0.7 to −0.6 m next to the mainland in the southwest portion of Biscayne Bay. In the case of the 1.05 m SLR, the spatial pattern of PSSH differences is similar to that for the case of 0.6 m SLR, except that the area with large negative differences in PSSH values becomes larger at the southeast corner of Biscayne Bay (Fig. 2c). The variations of PSSHs for various SLR scenarios at sample points 7 and 8 show that PSSHs increase in almost a linear fashion with slightly higher and lower rates than those for the linear combinations of SLR and storm surge (Fig. 3). This indicates that there is a weak nonlinear interaction between storm surge and SLR inside Biscayne Bay.

The strong nonlinear interaction occurs at the mainland by southern Biscayne Bay, where the PSSH differences range from 2.6 m to 3.7 m in some areas in the case of the 0.6 m SLR (Fig. 2b), resulting in 75–100 % changes in PSSHs compared to the case without considering nonlinear interaction. In the case of the 1.05 m SLR, the overall spatial pattern of PSSH differences over the mainland is similar to that in the case of the 0.6 m SLR, except
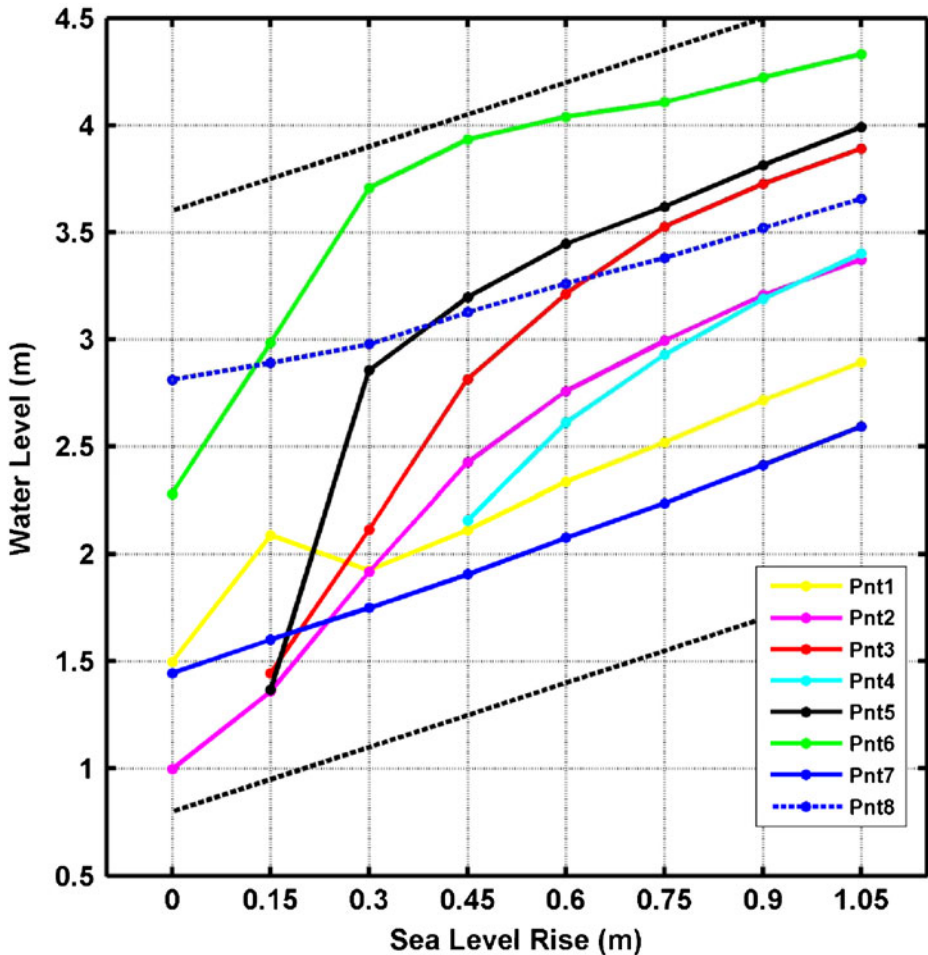
Fig. 3 Computed PSSHs by CEST at sample points in the study area as sea level rises. Two *black dashed lines* represent the linear combination of storm surges of 0.8 m and 3.6 m with SLR scenarios from 0 m to 1.05 m with an interval of 0.15 m. If there is no nonlinear interaction between storm surges and SLR, the surge height curves at sample points should be parallel to these two *dashed lines*

that the area with large positive differences in PSSH values next to southern Biscayne Bay enlarges and moves inland slightly (Fig. 2c). The changes of PSSHs versus various SLR scenarios at sample points 1–6 exhibit different and strong nonlinear interactions (Fig. 3). The significant nonlinear interactions at these sample points occur when the depths under rising sea levels are less than 0.6–0.75 m. As the water depths become larger than 0.75 m, the interaction between storm surge and SLR becomes linear. This indicates that the strong nonlinear interaction between storm surge and SLR at a particular location occurs in the initial SLR stage and the nonlinear interaction become weaker as the sea level rises higher. There is a threshold of 0.7 m beyond which the interaction between storm surge and SLR becomes linear.

The nonlinear interaction between storm surge and SLR causes large PSSH differences between the base case and the cases for elevated sea levels by moving the high PSSH zone

(Fig. 2a) further inland as sea level rises. In the case of the 0.6 m SLR, the PSSHs along Profile 1 (Fig. 2a) exhibit a convex shape, while the PSSHs for the base case are concave (Fig. 4a). The difference between the PSSHs derived by the numerical simulation and the simple linear addition methods range from 1.0 m to 1.5 m in the 1–10 km land section along Profile 1. It is noteworthy that the PSSHs from the simple linear addition method are slightly higher than those from the numerical simulation at the shoreline because the PSSHs there are simply elevated based on the SLR magnitude. The static linear addition method fails to reproduce the surge height reduction at the shoreline caused by the increase of the water depth (Mousavi et al. 2011) as sea level rises. These differences in spatial patterns of PSSHs demonstrate that it is not appropriate to estimate the PSSHs on the land at the initial stage of SLR by simply adding the SLR magnitude to the PSSHs for the base case. In the case of the 1.05 m SLR, the PSSHs from the numerical simulation along Profile 1 exhibit a convex shape similar to that for the case of the 0.6 m SLR, resulting in a difference between the PSSHs derived by the numerical simulation and the simple linear addition methods similar to that for the case of the 0.6 m SLR. Several abrupt changes in PSSHs for elevated sea levels occur in the 1–5 km section along Profile 1 because the simple linear addition method
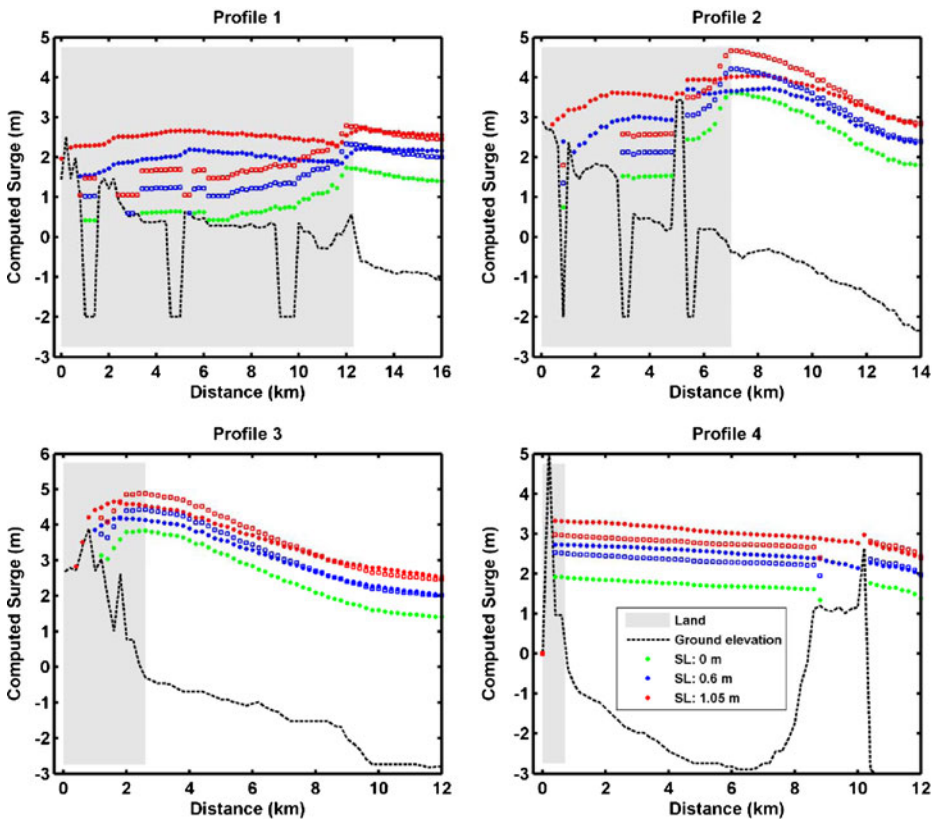

Fig. 4 The computed PSSHs for the current sea level (*green*), 0.6 m SLR (*blue*), and 1.05 m SLR (*red*) along four profiles. The PSSHs in the figure were derived by sampling computed PSSHs along a profile with an interval of 200 m. The *solid circle* represents the PSSHs computed by the CEST model, while the empty square represents the PSSHs derived by the simple linear addition method. Note that only the part of PSSHs along four profiles is displayed for the sake of clarity

estimates the PSSHs using elevated sea levels at the land area that are not inundated by base case storm surges. These abrupt changes disappear in the PSSHs generated by the linear addition by expansion method (Fig. 3a in SM Section 5). However, the differences between PSSHs from numerical simulations and the linear addition by expansion method are still large, and have an overall pattern similar to that for the differences between PSSHs from numerical simulations and the simple linear addition method.

The PSSH distribution shows a shorter inundation range on the land along Profile 2 than along Profile 1 (Fig. 4b and Fig. S3b). The differences between the PSSHs from numerical simulations and the PSSHs from the simple linear addition method range from 0.5 m to 1.2 m. The PSSHs generated by the simple linear addition method are about 0.8 m higher than that generated by the numerical simulation at the shoreline. The nonlinear effects become less obvious at Profile 3 as the inundation extent reduces along the coast of Biscayne Bay toward the north (Fig. 4c and Fig. S3c). The PSSHs generated by the simple linear addition method (0.2–0.4 m) are slightly higher than those generated using numerical simulations in the nearshore area. Profile 4 (Fig. 4d and Fig. S3d) shows the nonlinear interaction between storm surges and SLR in the northern Biscayne Bay. In the case of the 0.6 m SLR, the PSSHs generated by numerical simulations are 0.2 m above those generated by the simple linear addition method. In the case of the 1.05 m SLR, the differences between two PSSHs in the Bay increase slightly because more water is available for being pushed toward the northern Bay when the tail of Hurricane Andrew crosses the Bay.

The spatial differences in the interaction between storm surges and SLR were further examined in a regional scale for four regions including the open water next to Biscayne Bay, Biscayne Bay, the mainland by the Bay, and the barrier island including Miami Beach (SM Section 6 and Figs. S4-S9). The results show that the average PSSHs reduce slightly as sea level rises in Biscayne Bay and the open ocean outside Biscayne Bay, indicating a weak nonlinear interaction between storm surges and SLR. The average PSSHs for the mainland area by Biscayne Bay from numerical simulations are 22–24 % higher on average under various SLR scenarios than those from the simple linear addition and linear addition by expansion methods. The flooded areas from numerical simulations are 16–30 % larger on average than those from two linear addition methods. These differences can cause a large deviation in estimation of exposed population and property to storm surge flooding in the future (SM Section 7 and Figs. S10 and S11). In the case of the 1.05 m SLR, estimations of exposed population from numerical simulation, linear addition by expansion, and the simple linear addition methods differ by up to 50–140 % and estimations of exposed property differ by up to 20–80 %.

The average PSSHs and the flooded areas from the simple linear addition method differ from the values calculated based on the numerical simulations by 12 % and 30 % on average, respectively, over the barrier island including Miami Beach (Fig. S9). However, the average PSSHs and the flooded areas from the linear addition by expansion method and numerical simulations only differ by 4 % and 7 % on average, respectively. This indicates that the linear addition by expansion method closely approximates numerical simulations in estimating overland flooding in this area. For a given SLR scenario, the computation time of modeling storm surges based on a 100 h track is about 120 min by using a single 2.4 GHZ Intel Core i7-2760QM processor. By contrast, it takes less than 2 min and about 2–4 min for the simple linear addition and for the linear addition by expansion method, respectively, to complete the computation of flooding for a given SLR scenario using the same processor. Therefore, substantial computational effort will be saved in estimating storm surge flooding risk from a large number of hurricanes if numerical simulations can be approximated by the linear superimposition methods.

5 Discussion

A frequently used method to estimate the SLR effect on storm surges is to initially calculate the return periods of extreme water levels, which are the average durations of time between events that exceed a given level (McInnes et al. 2003), based on historical water level records. Then, the SLR effect on extreme water levels is estimated linearly by shifting the return period curve in terms of the SLR magnitude (Hallegatte et al. 2011; Kirshen et al. 2008; Tebaldi et al. 2012). The calculation of the return periods of extreme water levels using annual maxima from tide gauge records is a common practice in the design of coastal and offshore engineering projects (Pugh 1996). In this study, compared to PSSHs for the current sea level, the PSSHs with SLRs are reduced by 0.2 m in most open ocean areas outside Biscayne Bay. Although there are both increases and decreases in PSSHs inside Biscayne Bay under various SLR scenarios, the ranges of increase and decrease in most areas are limited to −0.2 to 0.2 m. Numerical simulations conducted for the North Sea also indicate that a 5 m SLR caused a change in storm surge heights of between −0.2 m and 0.1 m (De Ronde 1993). The study of storm surges at the open oceans around the United Kingdom showed that the effect of 0.5 m SLR was to change extreme water levels by approximately 0.45–0.55 m (Lowe et al. 2001; Lowe and Gregory 2005). Therefore, the estimation of the SLR effect on extreme water levels by directly adding the SLR magnitude to PSSHs is acceptable at tide gauges in the open coast where the nonlinear interaction between storm surge and SLR is weak.

However, a direct application of a return period curve from a tide gauge to the coastal area away from the gauge by assuming a similar interaction pattern for surge and SLR is problematic. First, the nonlinear interaction between storm surge and SLR in shallow water, especially in the inundated land area, can result in a significant under- or over-estimate of the magnitude of inundation at any specific location as shown in Fig. 4 and Fig. S3. Second, the distributions of extreme water levels change spatially because of the complicated interaction between storm surges and bathymetry/topography. For example, there are remarkable spatial changes in PSSHs from Hurricane Andrew along the Biscayne Bay Coast (Fig. 2a). McInnes et al. (2009) also found that 1-in-100 year storm surge heights change from low to high along the Australian Coast by Bass Strait with a difference of 0.8 m when they conducted hydrodynamic modeling of future storm surges with climate changes. Thus, the estimation of storm surge frequency is only effective for a specific location where water levels are recorded. The spatial variation of inundation magnitudes due to local topographic and land cover effects prevents the extrapolation of the estimate from a particular tide gauge to neighboring land areas. The appropriate way to estimate the return period of inundation magnitudes for a coastal area influenced by SLR will have to be generated from numerical simulations based on historical storm climatology using a well-calibrated surge model.

Two types of methods have been employed to estimate the impacts of storm surge flooding with SLRs. One is the linear addition of the SLR magnitudes to storm surge values over the land for the current sea level (Frazier et al. 2010; Kleinosky et al. 2007; Shepard et al. 2011; Wu et al. 2002). The other is the modeling of surge flooding based on hydrodynamic models with various scenarios of SLRs (McInnes et al. 2003, 2011). The numerical experiments of storm surge from Hurricane Andrew with a series of SLRs demonstrate that the nonlinear interaction between SLR and storm surge is strong for inundation and the inundation dynamics are not constant as assumed by the linear addition method. The inundation process changes as the surge flooding moves toward the inland as sea level rises because the bottom friction and wind surface stress are altered by spatial variations of land covers and topographic features. The change of inundation dynamics can amplify the magnitudes and extents of surge flooding as shown in the case for the mainland area by southern Biscayne Bay. Therefore, the utilization of the linear

addition method could lead to significantly underestimate affected population and property by storm surge flooding for a given SLR scenario.

6 Conclusions

There is a spatial variation in the interaction between storm surge and SLR that was demonstrated by modeling storm surge of Hurricane Andrew in the Miami Basin with a series of SLR scenarios. The weak linear interaction between storm surge and SLR occurs at the open ocean outside Biscayne Bay and PSSHs there reduce slightly as sea level rises. It is appropriate to estimate the SLR contribution to PSSHs by directly adding the SLR magnitude to PSSHs when an engineering project at the open coast and ocean is designed by considering the SLR effect. In Biscayne Bay, the nonlinear interaction between storm surge and SLR becomes slightly stronger than that in the open ocean. Overall, PSSHs with an elevated sea level at the northern portion of Biscayne Bay are slightly higher than the linear addition of the SLR to the base case storm surge for the current sea level, while PSSHs in the middle and southernmost portions of Biscayne Bay are slightly lower than those from the linear addition.

There is a strong nonlinear interaction between storm surge and SLR for the mainland area by Biscayne Bay. The variation of PSSHs from the shoreline toward inland caused by the shifting of the inundation zone as sea level rises leads to a large difference between the PSSHs for an elevated sea level and the base case PSSHs for the current sea level in the land area exposed to storm surge flooding. This large difference makes it inappropriate to use the linear addition methods to estimate the magnitude and extent of storm surge flooding for the land area affected by SLR. The difference can also lead to a large deviation in estimating population and property exposed to surge flooding induced by SLR. In the case of the 1.05 m SLR, the differences in estimations of exposed population derived using numerical simulation, linear addition by expansion, and the simple linear addition methods reach up to 50–140 % in this area. The interaction between storms surge and SLR at a specific location changes as sea level rises. The strong nonlinear interaction between storm surge and SLR occurs at the initial stage of SLR, while this interaction becomes linear after the water depth of the location is larger than 0.7 m. The utilization of a series of SLR scenarios to examine the interaction between storm surge and SLR not only accommodates the uncertainty in the projection of future SLR, but also allows the analysis of temporal changes of the interaction between storm surge and SLR at a specific location. This strategy is recommended to be used in the analysis of storm surge flooding induced by SLR in other coastal areas.

The linear addition by expansion method approximates the extent and magnitude of storm surge flooding from numerical simulations better than the simple addition method in the barrier island including Miami Beach. The flooded areas and peak storm surge heights generated by the linear addition by expansion method only differ from that produced by numerical simulations by 7 % and 4 % on average, respectively, while the simple linear addition method underestimates the flooded areas from numerical simulation by 30 % and peak surge heights by 12 % on average.

References

Bindoff NL, Willebrand J, Artale V, Cazenave A, Gregory J, Gulev S, Hanawa K, Le Quéré C, Levitus S, Nojiri Y, Shum CK, Talley LD, Unnikrishnan A (2007) Observations: oceanic climate change and sea level. In: Solomon S, Qin D, Manning M, Chen Z, Marquis M, Averyt KB, Tignor M, Miller HL (eds) Climate change 2007: the physical science basis. Contribution of working group I to the fourth assessment report of the intergovernmental panel on climate change. Cambridge University Press, Cambridge

Davis RA (1997) Geology of the Florida coast. In: Randazzo AF, Jones DS (eds) The geology of Florida. University Press of Florida, Miami, pp 155–168

De Ronde JG (1993) What will happen to The Netherlands if sea-level rise accelerates? Climate and sea level change: observations, projections and implications 322–335

Douglas BC (2001) Sea level change in the era of the recording tide gauge. In: Douglas BC, Kearney MS, Leatherman SP (eds) Sea level rise: history and consequences. Academic, San Diego, pp 37–64

Finkl CW, Warner MT (2005) Morphologic features and morphodynamic zones along the inner continental shelf of southeastern Florida: an example of form and process controlled by lithology. J Coast Res 79–96

Flather R, Williams J (2000) Climate change effects on storm surges: methodologies and results. Climate scenarios for water-related and coastal impacts 66–72

Frazier TG, Wood N, Yarnal B, Bauer DH (2010) Influence of potential sea level rise on societal vulnerability to hurricane storm-surge hazards, Sarasota County, Florida. Appl Geogr 30:490–505

Hallegatte S, Ranger N, Mestre O, Dumas P, Corfee-Morlot J, Herweijer C, Wood RM (2011) Assessing climate change impacts, sea level rise and storm surge risk in port cities: a case study on Copenhagen. Clim Chang 104:113–137

Jelesnianski CP, Chen J, Shaffer WA (1992) SLOSH: sea, lake and overland surges from hurricanes. Technical report NWS 48. NOAA, Washington, p 71

Katsman CA, Sterl A, Beersma J, van den Brink H, Church J, Hazeleger W, Kopp R, Kroon D, Kwadijk J, Lammersen R (2011) Exploring high-end scenarios for local sea level rise to develop flood protection strategies for a low-lying delta—the Netherlands as an example. Clim Chang 109:617–645

Kirshen P, Knee K, Ruth M (2008) Climate change and coastal flooding in Metro Boston: impacts and adaptation strategies. Clim Chang 90:453–473

Kleinosky LR, Yarnal B, Fisher A (2007) Vulnerability of Hampton Roads, Virginia to storm-surge flooding and sea-level rise. Nat Hazard 40:43–70

Lin N, Emanuel K, Oppenheimer M, Vanmarcke E (2012) Physically based assessment of hurricane surge threat under climate change. Nat Clim Chang 2:462–467

Lowe JA, Gregory J (2005) The effects of climate change on storm surges around the United Kingdom. Phil Trans R Soc A Math Phys Eng Sci 363:1313–1328

Lowe J, Gregory J, Flather R (2001) Changes in the occurrence of storm surges around the United Kingdom under a future climate scenario using a dynamic storm surge model driven by the Hadley Centre climate models. Clim Dyn 18:179–188

Mattocks C, Forbes C (2008) A real-time, event-triggered storm surge forecasting system for the state of North Carolina. Ocean Model 25:95–119

McInnes KL, Walsh JE, Hubbert GD, Beer T (2003) Impact of sea-level rise and storm surges on a coastal community. Nat Hazard 30:187–207

McInnes KL, Macadam I, Hubbert GD, O'Grady JG (2009) A modelling approach for estimating the frequency of sea level extremes and the impact of climate change in southeast Australia. Nat Hazard 51:115–137

McInnes KL, Macadam I, Hubbert G, O'Grady J (2011) An assessment of current and future vulnerability to coastal inundation due to sea level extremes in Victoria, southeast Australia. Int J Climatol

Mousavi ME, Irish JL, Frey AE, Olivera F, Edge BL (2011) Global warming and hurricanes: the potential impact of hurricane intensification and sea level rise on coastal flooding. Clim Chang 104:575–597

National Research Council (1987) Responding to changes in sea level: engineering implications. National Academy Press, Washington

Powell MD, Houston SH, Amat LR, Morisseau-Leroy N (1998) The HRD real-time hurricane wind analysis program. J Wind Eng Ind Aerodyn 77&78:53–64

Powell MD, Uhlhorn EW, Kepert JD (2009) Estimating maximum surface winds from hurricane reconnaissance measurements. Weather Forecast 24:868–883

Pugh DT (1996) Tides, surges and mean sea-level (reprinted with corrections). John Wiley & Sons Ltd

Rahmstorf S (2007) A semi-empirical approach to projecting future sea-level rise. Science 315:368–370

Sella GF, Stein S, Dixon TH, Craymer M, James TS, Mazzotti S, Dokka RK (2007) Observation of glacial isostatic adjustment in "stable" North America with GPS. Geophys Res Lett 34:L02306–L02307

Shepard CC, Agostini VN, Gilmer B, Allen T, Stone J, Brooks W, Beck MW (2011) Assessing future risk: quantifying the effects of sea level rise on storm surge risk for the southern shores of Long Island, New York. Nat Hazards 1–19

Smith JMK, Cialone MA, Wamsley TV, McAlpin TO (2010) Potential impact of sea level rise on coastal surges in southeast Louisiana. Ocean Eng 37:37–47

Tebaldi C, Strauss BH, Zervas CE (2012) Modelling sea level rise impacts on storm surges along US coasts. Environ Res Lett 7:014032

U.S. Army Corps of Engineers (2011) Sea-level change considerations for civil works programs. EC 1165-2-212, p. 32

Vermeer M, Rahmstorf S (2009) Global sea level linked to global temperature. Proc Natl Acad Sci 106:21527–21532

Wu SY, Yarnal B, Fisher A (2002) Vulnerability of coastal communities to sea level rise: a case study of Cape May County, New Jersey, USA. Clim Res 22:255–270

Zhang K (2011) Analysis of non-linear inundation from sea-level rise using LIDAR data: a case study for South Florida. Clim Chang 106:537–565

Zhang K, Douglas BC, Leatherman SP (2004) Global warming and coastal erosion. Clim Chang 64:41–58

Zhang K, Xiao C, Shen J (2008) Comparison of the CEST and SLOSH models for storm surge flooding. J Coast Res 24:489–499

Zhang K, Liu H, Li Y, Xu H, Shen J, Rhome J, Smith TJ III (2012) The role of mangroves in attenuating storm surges. Estuarine Coastal Shelf Sci 102–103:11–23